Higher Plant Photosystem II Light-Harvesting Antenna, Not the Reaction Center, Determines the Excited-State Lifetime—Both the Maximum and the Nonphotochemically Quenched

Erica Belgio,[†] Matthew P. Johnson,[‡] Snježana Jurić,[§] and Alexander V. Ruban[†*]

[†]School of Biological and Chemical Sciences, Queen Mary University of London, London, United Kingdom; [‡]Department of Molecular Biology and Biotechnology, University of Sheffield, Sheffield, United Kingdom; and [§]Division of Molecular Biology, Ruđer Bošković Institute, Zagreb, Croatia

ABSTRACT The maximum chlorophyll fluorescence lifetime in isolated photosystem II (PSII) light-harvesting complex (LHCII) antenna is 4 ns; however, it is quenched to 2 ns in intact thylakoid membranes when PSII reaction centers (RCIIs) are closed (Fm). It has been proposed that the closed state of RCIIs is responsible for the quenching. We investigated this proposal using a new, to our knowledge, model system in which the concentration of RCIIs was highly reduced within the thylakoid membrane. The system was developed in *Arabidopsis thaliana* plants under long-term treatment with lincomycin, a chloroplast protein synthesis inhibitor. The treatment led to 1), a decreased concentration of RCIIs to 10% of the control level and, interestingly, an increased antenna component; 2), an average reduction in the yield of photochemistry to 0.2; and 3), an increased nonphotochemical chlorophyll fluorescence quenching (NPQ). Despite these changes, the average fluorescence lifetimes measured in Fm and Fm′ (with NPQ) states were nearly identical to those obtained from the control. A 77 K fluorescence spectrum analysis of treated PSII membranes showed the typical features of preaggregation of LHCII, indicating that the state of LHCII antenna in the dark-adapted photosynthetic membrane is sufficient to determine the 2 ns Fm lifetime. Therefore, we conclude that the closed RCs do not cause quenching of excitation in the PSII antenna, and play no role in the formation of NPQ.

INTRODUCTION

Photosynthesis in eukaryotic organisms is encoded by the two distinct genomes of the nucleus and the chloroplast (1). The photosynthetic membrane of chloroplasts is the site for the primary conversion and storage of light energy. This process starts with the absorption of light quanta by the light-harvesting antenna pigments and transfer of the excited electron energy to the reaction centers of photosystems I and II (RCI and RCII, respectively), where primary charge separation occurs, and is followed by electron and proton transfer across the photosynthetic membrane, resulting in the formation of NADPH and ATP. Light-harvesting pigment-protein complexes (LHCs) serve as antennas to increase the spatial and spectral cross section of RCI and RCII, thereby increasing their photosynthetic efficiency. RCII is served by the LHCII antenna, which is formed by the major trimeric LHCIIs and the minor monomeric antenna complexes (CP24, CP26, and CP29), whereas RCI is served by the dimeric LHCIs (2). All light-harvesting outer antenna proteins are encoded by the nuclear genome, whereas the majority of RCI and RCII proteins are encoded by the chloroplast genome (3). The underlying reasons for this division of the antenna and RC proteins between the genomes remain the subject of much debate (4,5). A carefully orchestrated interaction between the two genomes is required for the response to changes in light quality and quantity because the amounts of RCs and LHCs must be carefully balanced to achieve optimal photosynthesis.

RCIIs are naturally susceptible to photo-oxidative damage that leads to a decrease in photosynthetic efficiency (photoinhibition) (6). Plants have evolved several mechanisms that are thought to protect against excess light. One is the dissipation of excess absorbed energy by PSII into heat, which can be measured as a decrease in the yield of chlorophyll fluorescence under light-saturating conditions and is known as nonphotochemical fluorescence quenching (NPQ) (7). Another mechanism is based on the repair of damaged RCIIs, which removes the D1 protein (the major site of damage within RCII) and replaces it with newly synthesized D1 (8,9). However, under excess light, the rate of D1 damage exceeds that of repair, leading to photoinhibition (10,11). The repair of D1 can also be inhibited by antibiotics, such as lincomycin, that inhibit chloroplast protein synthesis (11,12). The onset of photoinhibition can be monitored by pulse amplitude-modulated (PAM) chlorophyll fluorimetry and analysis of D1 levels (11). In studies of various aspects of photoinhibition, investigators have employed lincomycin treatment during measurements (11–16); however, little is known about the long-term application of lincomycin and its consequences on plant growth and photosynthetic membrane development. Early work that involved relatively short treatments with plastid protein synthesis inhibitors in greening beans and maize seedlings suggested a relative decrease in RCIIs and structural alterations that manifested as changes in the

Submitted March 8, 2012, and accepted for publication May 7, 2012.

*Correspondence: a.ruban@qmul.ac.uk

Editor: Leonid Brown.

0006-3495/12/06/2761/11 $2.00

doi: 10.1016/j.bpj.2012.05.004

distribution and abundance of the photosynthetic membrane proteins (17,18).

In this study, we watered *Arabidopsis* plants exclusively with a solution of lincomycin for several weeks to obtain an in vivo model system of membranes that had reduced amounts of RCs and were enriched in antenna complexes. This represents an interesting model for studies of the role of RCII in photoprotection and the character of the excitation energy trapping in this photosystem. We obtained well-established plants with an average Fv/Fm of 0.2, high levels of NPQ, and ~10% of the amount of control RCIIs in the photosynthetic membranes. Along with the biochemical characterization of the photosynthetic protein components, we conducted a careful spectroscopic study based on fluorescence lifetimes at Fm, conditions of dark-adapted closed reaction centers, and NPQ states (Fm′), and low-temperature fluorescence measurements on the system. Our findings suggest that, in principle, the proteolipidic environment of the photosynthetic membranes can be sufficient to determine the quenched 2 ns state that is usually observed for fluorescence of antennas at Fm. Taken together, the results indicate that the state of LHCII in the membrane is partially aggregated, compared with the detergent-solubilized one, and that despite the reduction in the number of RCs, the maximum fluorescence lifetime remains 2 ns. This implies that closed RCIIs play no role in quenching excitation within the antenna, or in the formation of NPQ.

MATERIALS AND METHODS

Plant growth

Arabidopsis thaliana (L.) Heynh. ecotype Columbia (*Arabidopsis*) was grown for 10 weeks in Sanyo plant growth cabinets with an 8-h photoperiod at a light intensity of 100 μmol photons m^{-2} s^{-1} and a day/night temperature of 22/15°C. Lincomycin (0.1 g/L; Sigma Aldrich, Munich, Germany) was added to the irrigation water starting from the rosette stage and continued until the whole-plant stage. All measurements were performed on leaf areas where Fv/Fm was in the range of 0.1–0.3.

SDS-PAGE and Western blot

The concentration of proteins in total extracts obtained from *Arabidopsis* leaves was determined and normalized according to Bradford (19). The proteins were resolved by SDS-PAGE in 12% acrylamide gel and transferred onto nitrocellulose membrane. Immunoblotting was performed by incubation with primary antibodies specific for *Arabidopsis* D1, Lhcb1,2,3 (LhcbII) and Lhcb4 (CP29), Lhcb5 (CP26), Lhcb6 (CP24), PsaA and Lhcba2, and PsbS protein (Agrisera, Sweden). TROL (a rhodanese-like protein responsible for docking of ferredoxin-$NADP^+$ reductase to the thylakoids) antibody was a kind gift from Prof. H. Fulgosi. Detection was performed with the use of the ECL Plus Western Blotting Detection System (GE Healthcare Life Sciences, UK). Densitometry of the immunosignals was done using NIH ImageJ software and associated plugins (http://rsb.info.nih.gov/ij/), taking the wild-type level as 100% and using anti-TROL antibody as a control for the lane loading. The percentages reported in the Results section are the average of five to 10 different samples.

Fast protein liquid chromatography analysis of thylakoid membranes

Fast protein liquid chromatography (FPLC) analysis was performed on detergent-solubilized, freshly prepared, stacked thylakoid membranes as described previously (20). The thylakoids were suspended to a final chlorophyll concentration of 1.0 mg/mL and partially solubilized by the addition of *n*-dodecyl α-D-maltoside to a final concentration of 1% and incubated for 1 min at room temperature. Unsolubilized material was removed by 1 min of centrifugation at 16,000 × *g*. The supernatant was then filtered through a 0.45-μm filter and subjected to gel filtration chromatography on an Amersham-Pharmacia Äcta purifier system, including a Superdex 200 HR 10/30 column.

Pigment analysis

The total pigments were extracted from leaves after incubation on 80% ice-cold acetone and 5 min centrifugation in a bench centrifuge at maximum speed. Absorbance at 646.6, 663.6, and 750 nm was detected to determine the total chlorophyll concentration and chlorophyll *a/b* ratio, calculated according to Porra et al. (21). Zeaxanthin and the de-epoxidation state (zeaxanthin + 0.5*antheraxanthin)/(violaxanthin + antheraxanthin + zeaxanthin) were determined by reversed-phase high-performance liquid chromatography using a LiChrospher 100 RP-18 column (Merck) and a Dionex Summit chromatography system as previously described (22).

Chlorophyll fluorescence induction

Chlorophyll fluorescence was measured with a Dual PAM 100 chlorophyll fluorescence photosynthesis analyzer (Heinz Walz). Plants were adapted in the dark for 30 min before measurements were obtained. Actinic illumination of 200 and 700 μmol photons m^{-2} s^{-1}, respectively (see the Results section), was provided by arrays of 635-nm LEDs illuminating both the adaxial and abaxial surfaces of the leaf. Fo (the fluorescence level with open RCIIs) was measured in the presence of the 10 μmol photons m^{-2} s^{-1} measuring beam. Maximum fluorescence in the dark-adapted state (Fm) during the course of actinic illumination (Fm′) and in the subsequent dark relaxation periods was determined using a 0.8 s saturating light pulse (1000 μmol photons m^{-2} s^{-1}). We defined the quantum yield of PSII (Fv/Fm) as ((Fm − Fo)/Fm); NPQ as ((Fm − Fm′)/Fm′); and qP as ((Fm′ − Fs)/Fo), where Fs is the steady-state fluorescence level.

Fitting NPQ kinetics

NPQ formation data were fitted with a Hill function $NPQ(t) = NPQ_{max}t^b/(t_{0.5}{}^b + t^b)$ using SigmaPlot software (SPSS, Chicago, IL), where NPQ_{max} is the maximum NPQ amplitude, $t_{0.5}$ is the *t*-value at which NPQ = 50% of NPQ_{max}, and *b* is the sigmoidicity parameter; thus $(1/t_{0.5})$ is the rate of NPQ formation. NPQ relaxation data were fitted with a hyperbolic decay $NPQ(t) = NPQ_0 + NPQ_{max}\ t'_{0.5}\ /(t'_{0.5} + t)$, where NPQ_{max} is the starting NPQ amplitude, $t'_{0.5}$ is the *t*-value at which NPQ = 50% of NPQ_{max}, and NPQ_0 is the amplitude of NPQ that does not relax within 300 s; thus, $1/t'_{0.5}$ is the rate of NPQ relaxation.

Measurements of chlorophyll fluorescence lifetime

Time-correlated single photon counting (TCSPC) measurements were performed on a FluoTime 200 ps fluorometer (PicoQuant, Germany). Detached leaves were vacuum-infiltrated with 50 μM nigericin to completely inhibit NPQ. Excitation at the 10 MHz repetition rate was provided by the 470 nm laser diode, which was carefully adjusted to completely close all RCIIs without causing photoinhibitory quenching of Fm, and to be far below

the onset of singlet-singlet exciton annihilation. For the measurements of Fm′ values, NPQ was induced in leaves infiltrated with water with 200 (lincomycin-treated) or 700 (untreated) μmol photons m^{-2} s^{-1} by arrays of 635 nm LEDs. Fluorescence was detected at 682 nm on leaves with the 2 nm slit width. The instrumental response function was in the range of 50 ps. For lifetime analysis, FluoFit software (PicoQuant) was used. The quality of the fits was judged by the χ^2 parameter. In addition, the autocorrelation function of the weighted residual data was obtained as a measure of the correlation between the residuals in distinct channels separated by various times. Because the residual values should be normally distributed in the good fit (not correlated), the autocorrelation data were randomly distributed around zero and their fluctuations were small. We also performed a support plane analysis by calculating χ^2 as a function of each single parameter to estimate the region of the function below the tolerance level. Intensity-weighted average lifetimes were calculated as $\sum (A^*\tau)/\sum A$, and amplitude averages were calculated as $\sum (A^*\tau^2)/\sum (A\ \tau)$.

Steady-state fluorescence spectroscopy

For all fluorescence measurements, leaf homogenates were carefully prepared and diluted to avoid reabsorption (23) in 10 mM Hepes buffer, pH 7.6. Low-temperature (77 K) emission spectra were recorded on a Jobin Yvon FluoroMax-3 spectrophotometer equipped with a liquid-nitrogen-cooled cryostat. Excitation was defined at 435 nm with the 5 nm spectral bandwidth. The fluorescence spectral resolution was 1 nm. Spectra were normalized at their absolute maximum. The second derivative analysis was calculated after a smoothing of the spectrum (FFT filter of the Originlab program) with a wavelength interval of 3 nm.

LHCII isolation

Spinach trimeric LHCIIb was isolated as previously described (22). LHCII was desalted in a PD10 desalting column (GE Healthcare) in a buffer containing 20 mM Hepes (pH 7.8) and 0.03% (w/v) *n*-dodecyl β-D-maltoside (β-DM). Aggregated LHCII was prepared by removal of detergent by SM-2 bioabsorbent beads (Bio-Rad) producing reduction in fluorescence average lifetime (see below) from 4 ns to 2 ns.

Isolation of PSI

PSI complex was isolated by sucrose gradient ultracentrifugation as previously described (20). Briefly, unstacked thylakoids were treated on ice for 30 min with 1% β-DM with a ratio of β-DM/chl of 10. Sucrose gradients were seven-step exponential gradients from 0.15 to 1.0 M sucrose dissolved in 20 mM Hepes buffer containing 20 μM β-DM. The run time was 18 h at 200,000 $\times$ g in an SW41 rotor at 4°C.

RESULTS

Growth with lincomycin highly enriches the photosynthetic membrane in LHCs

Lincomycin was selected from other antibiotics because it has been found to be a more specific inhibitor of plastid protein synthesis (14,16). The treatment, conducted as described in the Materials and Methods section (also see Supporting Material), induced a heterogeneous phenotype characterized by a decrease in the Fv/Fm ratio and a general reduction in chlorophyll concentration by 40% on average (Table S1). The growth rate of the treated plants was affected, but despite this they were able to reach the flowering stage. To study membranes with the greatest reduction in RCs, we used only leaves with Fv/Fm in the range of 0.1–0.3.

We analyzed the effect of lincomycin treatment on the photosynthetic membrane protein components by immunoblotting total leaf extracts against D1 and Lhcb1-6 antibodies (a representative result is shown in Fig. 1). An antibody against TROL, a nuclear-encoded protein that is not directly influenced by lincomycin treatment (24), was used as a control for loading. In similarity to previous observations from maize (18), the level of D1 was strongly decreased (12% ± 4%), whereas the level of the major LHCII polypeptides, Lhcb1 and Lhcb2, was increased (160% ± 10%). In the minor antennas, Lhcb5 and Lhcb6 remained mainly unaffected, whereas Lhcb4 (CP29) was reduced. Interestingly, the levels of the minor constituent of the trimeric LHCII complex, Lhcb3, also remained unaffected. These results indicate that the composition and organization of PSII in treated plants were markedly changed, and that different, perhaps inversely related, feedback mechanisms regulate nuclear gene expression for the major LHCII polypeptides and CP29. Previously, similar results were obtained using low temperature, a treatment that reduced RCII accumulation and increased LHCII but not CP29 (25). CP29 is closely associated with the RCII core complex and is one of the key complexes required to stabilize the PSII supercomplex structure (26). It has also been suggested to have a crucial role in energy transfer

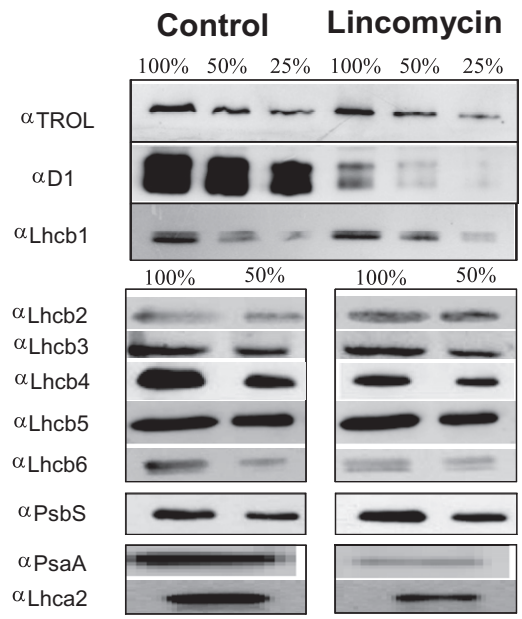

FIGURE 1 Representative Western blot result showing the polypeptide composition of *Arabidopsis* plants grown with lincomycin. Total protein extracts from leaves were loaded in equal amounts (100% = 10 μg of total protein per lane), detected using designated antibodies, and analyzed as described in Materials and Methods.

from the antenna to the RC (27). Therefore, a possible explanation for the different regulation is that its expression and incorporation into the photosynthetic membrane is at least partially dependent on the PSII assembly.

To further address the photosynthetic membrane composition, we prepared stacked thylakoids from leaves, solubilized them with *n*-dodecyl α-D-maltoside (α-DM), and applied them to a gel filtration column as previously described (20). Gel filtration is a gentle and incisive way to separate different green complexes on the basis of size (larger complexes elute first). FPLC elution profiles from the control and lincomycin-treated plants are shown in Fig. 2. The achievement of almost complete membrane solubilization is evidenced from the low amplitudes of peaks I and II, where PSII membrane fragments and supercomplexes are normally found. The treated membranes contained low amounts of PSII core complexes (<20% of control, as quantified by calculating the area under the relative subband; Fig. S1), whereas band V, which normally carries LHCII trimers (here verified by an absorption spectrum; Fig. 2, *inset*), dominated the results and was estimated to be 150% that of control, in agreement with the Western blot quantification (Fig. 1). The consistency in results obtained with the two biochemical approaches clearly demonstrates that there was a significant increase in the amounts of the major LHCII, a fairly unchanged quantity of minors, and a strong decrease in the amount of RCs.

Interestingly, the FPLC profile showed an overall reduction in PSI complexes (19% with respect to the control; Fig. 2). Further investigation by Western blotting revealed that levels of the core PSI polypeptide, PsaA, as well as Lhca2, one of the LHCI group antennas, were reduced in the treated plants (Fig. 1). These findings are consistent with the FPLC results and substantiate the hypothesis that compared with PSII, expression of the RC and antenna components of PSI are more tightly interrelated and equivalent in expression. Indeed, although the LHC/RC ratio for PSI remained almost unchanged, that for PSII increased by up to ~10-fold compared with the control, corresponding to an increase in the PSII antenna/RC chlorophyll ratio from ~250 in the control to ~3000 in the treated plants. The big increase in the LHCII/RCII ratio was concordant with the calculated chlorophyll *a/b* ratio of 2 in the treated leaves, and 3 in the control (Table S1).

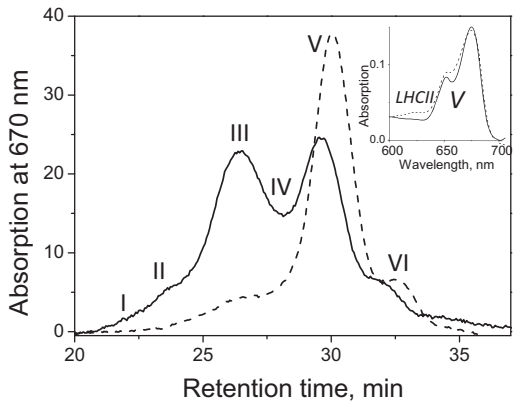

FIGURE 2 FPLC gel filtration fractionation of solubilized control (*solid line*) and treated (*dashed line*) thylakoid membranes. Major fractions are marked as follows: PSII membrane fragments (I), PSII supercomplexes (II), PSI complex (III), PSII core complexes (IV), trimeric LHCII (V), and monomeric minor LHCIIs (VI). Thylakoids were solubilized with 1% α-DM. The top-right inset shows the absorption spectrum of fraction V (*solid line*) compared with the spectrum of the isoelectric focusing-prepared major LHCII complex (*dashed line*).

Xanthophyll composition in treated plants

The zeaxanthin levels in the treated plants were the same as in the control, both before and after illumination, with the exception of a slightly higher level of antheraxanthin in the dark (not shown), which is reflected in the de-epoxidation state calculation.

Consequences of antenna enrichment on energy transfer in vivo: escape of excitation from trapping and high levels of NPQ

Fig. 3 presents typical PAM fluorescence induction traces of the control and treated plants exposed to 2 × 5 min 200 μmol photons m^{-2} s^{-1} actinic light illumination periods, each followed by 5 min of dark relaxation. Fluorescence levels when all RCIIs were in the open state (Fo) were much higher than in the control, suggesting that the remaining RCs were unable to quench the fluorescence of the antenna complexes with the same efficiency as the control, thus bringing Fo near the level of Fm. Similar results were previously obtained in experiments with maize plants treated for 72 h with lincomycin (18). The escape of a large proportion of excitation from the RC traps, which in turn affected the maximum efficiency of RCII (Fv/Fm), could be explained by the presence of an antenna population not energetically coupled to RCs. We investigated this hypothesis by obtaining fluorescence induction measurements of 3-(3,4-dichlorophenyl)-1,1-dimethylurea (DCMU)-infiltrated leaves of treated and control plants (Fig. 4). This method gives information on the functional size of the PSII antenna because the fluorescence rising time from Fo to Fm is inversely proportional to the antenna/RC chlorophyll ratio. Lincomycin-treated plants showed a faster rise in fluorescence induction, which we quantified as described previously (28) by calculating the area enclosed between the fluorescence curve [F = F (*t*)], the (vertical) axis ($t = 0$), and the maximal fluorescence horizontal line (F = Fm), where the value of the variable fluorescence (Fm − Fo) was normalized to unity (Fig. 4 *B*). As a consequence of a 30% decrease in the rise time, the functional antenna size in treated plants was estimated to be ~30% larger than that of the control, and therefore, taking into account the

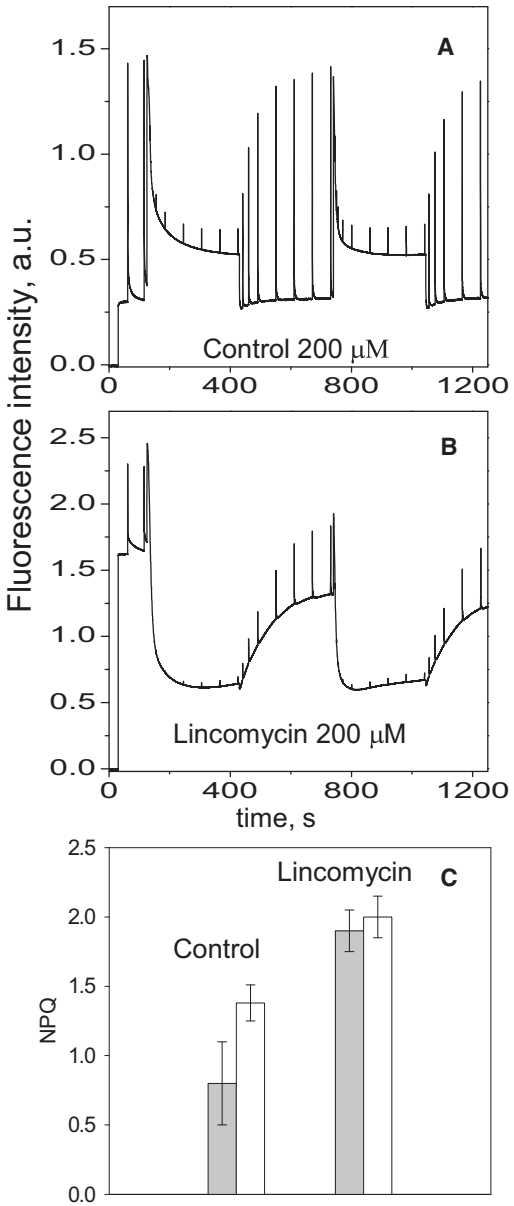

FIGURE 3 PAM chlorophyll fluorescence analysis of untreated (*A*) and treated (*B*) *Arabidopsis* leaves. (*C*) NPQ measured with 200 μmol photons m^{-2} s^{-1} illumination (*gray bar*) or 700 μmol photons m^{-2} s^{-1}(*white bar*) in control and treated plants after the second illumination cycle. Data are means ± SE from three replicates.

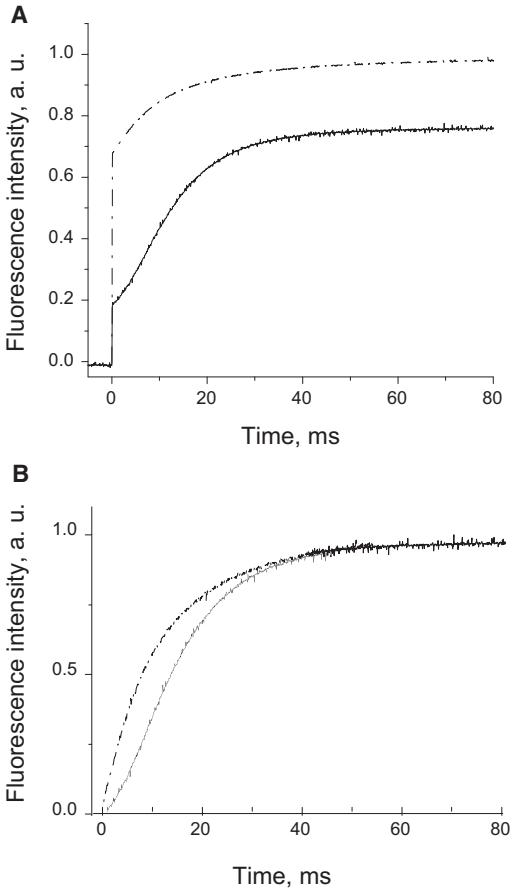

FIGURE 4 Induction of chlorophyll fluorescence at room temperature from untreated (*continuous line*) and lincomycin-treated (*dashed line*) *Arabidopsis* leaves. (*A*) Original fluorescence induction traces. (*B*) Normalized fluorescence induction traces to Fv = 1. The area above the induction curve is reciprocal to the antenna cross-section size. This area is larger for the control than for the treated sample. The difference corresponds to the PSII antenna cross-section increase in the treated samples by ~30%. Fluorescence induction kinetic traces were measured with PAM 100 in fast kinetics mode, providing a flash of light of 10 μmol $m^{-2}s^{-1}$ intensity after infiltration of the leaf with 30 μM DCMU, 150 mM sorbitol, and 10 mM Hepes, pH 7.5.

250:1 antenna/RCII chlorophyll ratio of the control, this ratio for the treated plants should be at maximum 325:1. Hence, we estimated that of the ~3000 chlorophylls, only 325 are functionally connected to the RCII in the lincomycin-treated plants, whereas the remaining 80–90% constitute a bed of chlorophylls uncoupled from the RCs, which gives rise to the corresponding increase in Fo (Fig. 3).

In addition to the increase in Fo, the PAM fluorimetry traces also showed the ability of lincomycin-treated plants to form NPQ and to quench Fo by more than two times (Fig. 3). Photochemical quenching (qP) was still detectable in lincomycin-treated plants during low actinic light illumination (200 μmol photons m^{-2} s^{-1}) and had a similar extent compared with the control, measured at 700 μmol photons m^{-1} s^{-1}, when both were normalized to their relative Fv/Fm values (compare Fig. 3 and Fig. S2). The need for a lower light intensity to attain similar qP levels was interpreted to be due to the somewhat increased cross section in lincomycin-treated plants. In these light conditions, a higher total amount of NPQ was brought about (Fig. 3 *C*) with similar rates of formation (Fig. S3, *A* and *B*), whereas the relaxation rate was lower (Fig. S3, *C* and *D*). Because the levels of PsbS protein were found to be similar to the control (see Fig. 1), and no changes in the xanthophyll cycle activity were detected (Table S1), the differences in the amount and rates of NPQ relaxation cannot be attributed to these components of NPQ. On the other hand, the

observed increase in NPQ is consistent with previous observations made on plants with a reduced size of the peripheral LHCII antenna. Indeed, plants grown under intermittent light or mutants lacking chlorophyll *b* were reported to possess lower levels of NPQ, suggesting that the peripheral LHCII is largely involved in photoprotection (29,30).

The choice of different actinic light intensities for the fluorescence induction in the treated and control plants was also reasoned on the basis of the extent of photoinhibition estimated from the 1-qP parameter as measured in the dark after the cycle of illumination, being an indicator of the fraction of damaged PSII centers (7,31). The light intensity of 200 μmol photons m^{-1} s^{-1} caused a similar extent of damage to the treated plants as to the untreated ones with 700 μmol photons m^{-1} s^{-1} (Fig. S4). Hence, the excitation pressure was considered to be equalized in these conditions.

The chlorophyll fluorescence lifetime of LHCII-enriched membranes is similar to that of the control in both light-harvesting and photoprotective states

It is known that a limited range of lifetimes can be found in vivo in leaves, where the average maximum lifetime does not exceed 2 ns and arises from the closure of RCIIs (32–38). At the other extreme is the NPQ state, in which the chlorophyll fluorescence lifetime is usually reported to be ~0.6–0.8 ns (32–34,36,38). Several reports (33,39) have indicated that the closed state of RCs is responsible for the 2 ns lifetime of the antenna at Fm, a fluorescence state that is quenched compared with the 4 ns detergent-solubilized antenna state. Because a decrease in the concentration of the quencher molecule is expected to have the consequence of increasing the average fluorescence lifetime, the treated plants with a low amount of RCs constituted an interesting sample for testing the above suggestion. Fig. 5 *A* displays chlorophyll fluorescence lifetime decay traces measured at 683 nm in control and treated leaves. The data for control leaves are in agreement with previous results (33,39,40). The intensity-weighted fluorescence lifetime of a control leaf at Fm was ~2 ns due to the presence of three decay components: 2.5 ns and 1.3 ns, both of 20–30% amplitude, and a third component of 100 ps, associated with PSI (Fig. 5 *B*). Induction of NPQ resulted in a decrease in the average fluorescence lifetime to ~0.8 ns, mainly due to shortening of the two longer lifetimes to 1.5 and 0.6 ns, respectively (Fig. 5 *C*). Remarkably, despite the dramatic differences in the LHCII antenna/RCII ratio, the average chlorophyll fluorescence lifetimes were found to be almost identical in both Fm and NPQ states in lincomycin-treated plants (Fig. 5 *A*, *black and red traces*). However, differences were evident in the component amplitudes at Fm (Fig. 5 *B*), predominantly due to the strong reduction in the fast decay component associated with PSI. This is consistent with the loss of this photosystem as a result of lincomycin treatment

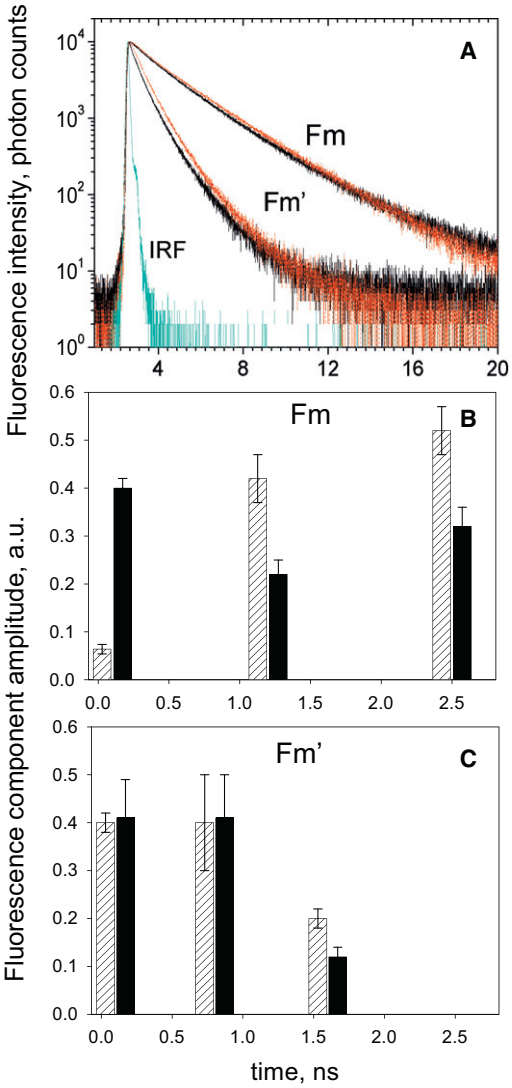

FIGURE 5 TCSPC analysis of the chlorophyll fluorescence lifetime in *Arabidopsis* leaves in harvesting and photoprotective states. (*A*) Chlorophyll fluorescence lifetime decay traces of control (*black*) and treated (*red*) *Arabidopsis* leaves. The light-harvesting (Fm) state (vacuum-infiltrated with 50 μM nigericin) is shown in comparison with the photoprotective (Fm′) state measured in the presence of 200 and 700 μmol photons m^{-2} s^{-1} of light, for treated and untreated plants, respectively. (*B* and *C*) Relative time-resolved fluorescence lifetime component amplitudes of control (*black*) and treated (*dashed*) leaves in the Fm (*B*) or Fm′ (*C*) states. Average intensity-weighted lifetimes: control Fm 2.0 ± 0.1 ns, lincomycin Fm 2.2 ± 0.1 ns, ct NPQ 0.9 ± 0.1 ns, lincomycin NPQ 0.8 ± 0.1 ns. Fluorescence was detected at 683 nm using a 470 nm excitation wavelength. Data are means ± SE from four replicates. IRF, instrument response function.

(see Fig. 1, *bottom*). However, because PSI contributes only 1% of total emitted photons, the intensity-weighted analysis did not yield significantly different average lifetimes in the two sets of plants. The average fluorescence lifetimes calculated for the PSII-only fraction were 2.13 ± 0.05 ns and 2.20 ± 0.10 ns in treated and control plants, respectively. Furthermore, the average fluorescence lifetimes in the Fm′

state at NPQ were 0.9 ± 0.1 and 0.8 ± 0.1 for control and treated plants, respectively. This result is fairly consistent with the levels of NPQ observed for the both types of plants.

Our findings suggest that the proposed extent to which closed RCIIs modulate the antenna chlorophyll lifetime should be reevaluated to account for the quenching effects of the proteolipidic membrane environment on the state of LHCII. In fact, it was previously shown that the LHCII fluorescence lifetime in liposomes at high protein/lipid ratios was not 4 ns, as for isolated trimers, but 2 ns (41), and an increasing number of studies are pointing to the effect of detergents on protein conformations, leading to different quenching states (42,43). It is therefore possible to consider that the 4 ns lifetime is an artificial condition that is induced by the detergent-aqueous environment and does not occur in vivo.

77 K fluorescence measurements show a partially aggregated state of LHCII antenna in the photosynthetic membrane

Finally, we measured the low-temperature emission spectra of leaf homogenate corresponding to the Fm state (Fig. 6). The spectrum of the treated leaf was 3–5 nm blue-shifted relative to that of the control, in both the PSII and PSI emission regions, with the two emission maxima at 682 nm and 730 nm, respectively. The second derivative of the spectra revealed strong changes in the PSII emission region (Fig. 6 *B*). The peaks at 680, 685, and 695 nm that are normally present in the control spectrum were largely absent from the spectrum of the treated sample, with only one dominating peak at 682 nm, similar to that obtained from the lincomycin-treated maize leaves (18). Although the 3 nm shift in PSII emission, from 685 to 682 nm, could be explained by the presence of emission from a large amount of free LHCII antenna, peaking at ~680 nm, it is somewhat more difficult to explain the elevation in the emission region above 690 nm (Fig. 6 *A*). The identity of the 696–705 nm band could be explained by 1), an emission from the CP47 core complex of PSII (44,45); 2), fluorescence from an LHCI antenna complex built of Lhca2 and 3 polypeptides (46); or 3), an F700 band of aggregated LHCII (47). The fact that the 696–705 nm region was strongly elevated in the lincomycin-treated plants contradicts the >10-fold decrease in RCII complexes if this emission were coming from the core complex. Therefore, the first explanation of its origin seems to be unlikely. The origin from LHCI is also not feasible, because the amount Lhca2 polypeptide and consequently that of Lhca3 (46) is also strongly reduced in treated plants (see Fig. 1). In addition, free LHCI should reveal strong fluorescence in the 696–705 nm region at room temperature (46), which is not the case according to Fig. 6 *C*, where the spectra of both control and treated plants are almost identical. Finally, the 77 K excitation fluorescence spectrum of this emission region was identical to that for 680 nm band and highly enriched in chlorophyll *b* (the peak around 472 nm; Fig. 6 *D*). This observation excludes the origin of 696–705 nm emission from LHCI and indicates that both the 680 nm and 696–705 nm emissions originate from the major LHCII complex.

To further investigate the nature of the 696–705 nm fluorescence in the treated plants, we subtracted the spectrum of a preparation of PSI (Fig. 6 *A*, *dotted line*) from the spectrum of the treated leaf homogenate. The difference spectrum represents the emission from PSII membranes only (Fig. 7 *A*, *top trace*). A maximum at 682 nm with a shoulder at 698 nm is apparent, a structure that is commonly found and has been reported to be proportional to the aggregation state of isolated antenna complexes, both major LHCII and

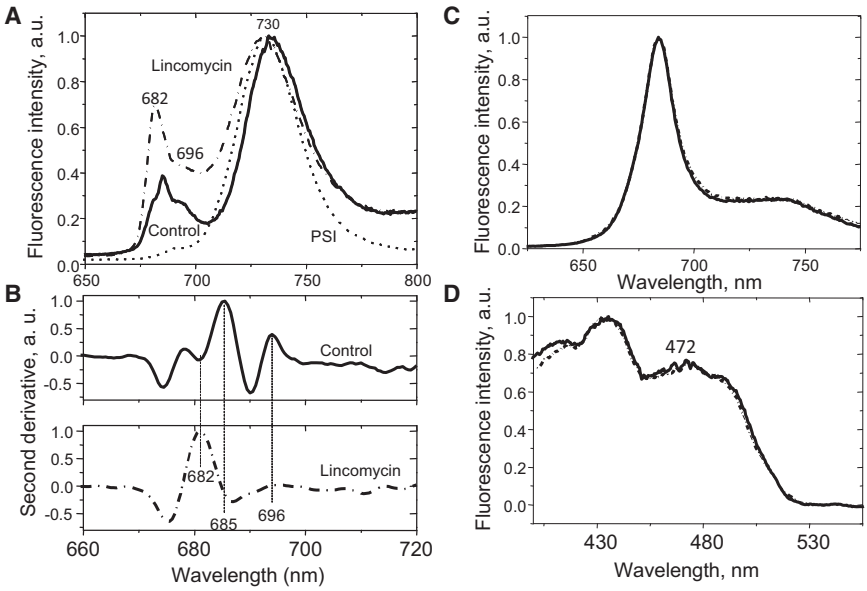

FIGURE 6 Fluorescence spectroscopy analysis of the changes in the state of the photosynthetic membrane induced by lincomycin. (*A*) The 77 K fluorescence spectrum of leaf homogenate from untreated (*solid line*) and treated (*dash-dotted line*) leaves. A PSI spectrum is shown for comparison (*dotted line*). (*B*) The second derivative of untreated (*solid line*) and treated (*dash-dotted line*) 77 K fluorescence spectra. (*C*) Room-temperature spectra of diluted leaf homogenates of the control (*solid line*) and lincomycin-grown (*dashed line*) plants. (*D*) 77 K excitation fluorescence spectra for 680 nm (*solid line*) and 700 nm (*dashed line*) bands of leaf homogenates from treated plants.

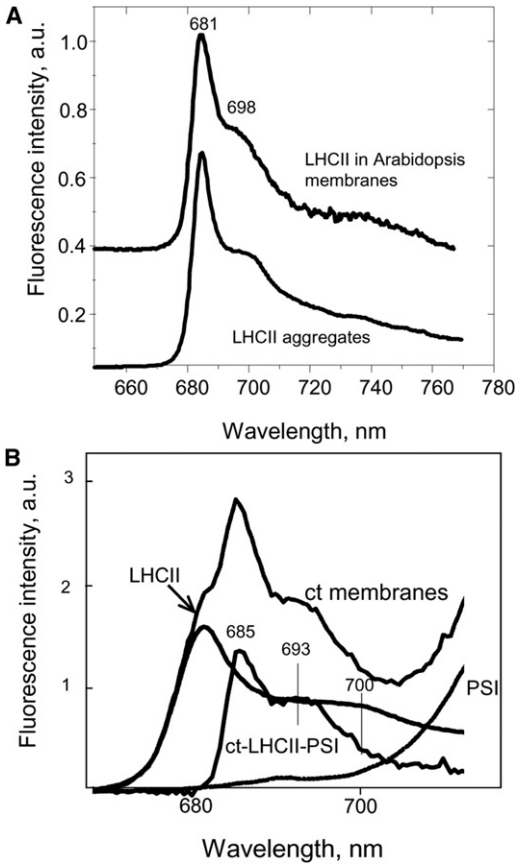

FIGURE 7 Low-temperature fluorescence spectral analysis of leaf homogenates. (*A*) Comparison between the fluorescence spectrums of treated leaf homogenate from which PSI spectrum was subtracted (*upper curve*) and the spectrum of aggregated LHCII with an average 2 ns lifetime. (*B*) The 77 K fluorescence spectra of control membranes (ct), aggregated LHCII with ~2 ns fluorescence lifetime (LHCII), isolated PSI (PSI), and a difference ct-minus-LHCII-minus-PSI spectrum (ct-LHCII-PSI).

minor complexes (CP24, CP26, and CP29) (48). Fig. 7 *A* shows the 77 K fluorescence spectrum of isolated and partially aggregated LHCII (~2 ns lifetime, *dot-dashed line*). The spectrum is remarkably similar to that of the PSII membranes (Fig. 7 *A*). This suggests that the LHCII antenna in vivo is partially aggregated and therefore quenched. To refine this point, we analyzed the fluorescence spectrum of the control in a similar way. The spectrum for LHCII aggregates with 2 ns average fluorescence lifetime, and the spectrum of isolated PSI was carefully subtracted from the spectrum of control membranes (Fig. 7 *B*). The spectral normalization criteria were simply chosen by using the standard curve-fit approaches. Fig. 7 *B* displays the resulting difference spectrum with 685 nm and 693 nm maxima. These are the typical features of the purified PSII core complex originating from the inner antenna CP43 and CP47 complexes, respectively (45–47). Therefore, we concluded that the LHCII antenna is likely to be in partially quenched, aggregated state also in the control thylakoid membranes, having a pronounced shoulder at 700 nm in its 77 K fluorescence spectrum that is usually masked by the emission from both RCIIs and PSI core antennae. The finding of an aggregated and partially quenched state of LHCII in the photosynthetic membrane confirms our earlier hypothesis regarding the oligomerization and dissipation state of LHCII in vivo (49).

DISCUSSION AND CONCLUSIONS

Here, we used two independent approaches, Western blotting and gel filtration, to show that inhibition of chloroplast translation due to prolonged treatment of plants with lincomycin results in membranes with a >10-fold reduction in the RCII/LHCII chlorophyll ratio. This provided an interesting model to study the structure and light-harvesting and photoprotective functions of the photosynthetic membrane. In the treated plants, the amount of major LHCII complex was increased, whereas in the minor CP29 complex, it was decreased. The latter is closely associated with the RCII core complex and is one of the key complexes that are required to stabilize the PSII supercomplex structure and have been suggested to have a crucial role in transferring energy from antenna to RCs (26,27). Interestingly, >90% of the RCII decrease was accompanied by a decline of only ~40% of CP29. This shows that the CP29/RCII ratio in membranes from treated plants is almost an order of magnitude higher than in the control plants. The obvious implication of such a strong alteration is that the expression and incorporation of CP29 into the photosynthetic membrane are relatively independent of the RCII assembly. It is also possible that in vivo, the PSII supercomplex structure is less rigid and more functionally dynamic than previously thought.

Although the membranes of treated plants were antenna-rich, only a low percentage of the antennas (10–20%) were estimated to be energetically coupled to the RCIIs. On the basis of the Fo to Fm induction time, this fraction was found to yield an antenna cross section 30% larger than that of the control. As a consequence, a large bed of uncoupled LHCII surrounded the few functional photosystems, providing an explanation for the high Fo levels and the consistent reduction of the Fv/Fm ratio, resulting from the escape of a large proportion of LHCII fluorescence from the RCII traps.

A surprising discovery was made during the measurements of the Fm fluorescence lifetime in the treated plants. Unexpectedly, the average PSII lifetime was almost the same as in the wild-type membranes, indicating that the LHCII antenna must be in a partially quenched state compared with the almost perfect monoexponential (4 ns) unquenched state of detergent-solubilized complex. We confirmed this by calculating the PSII membrane spectra of the lincomycin-treated plants and fitting the wild-type spectrum with a spectrum of partially quenched, aggregated LHCII with an ~2 ns fluorescence lifetime. This discovery suggests that closed RCIIs play a small role in modulating

the chlorophyll excited-state lifetime in the PSII-containing photosynthetic membrane. Previously, Holzwarth et al. (50) and Miloslavina et al. (51) proposed the so-called excited-state radical pair equilibrium (or trap-limited) model, according to which exciton equilibration between all antenna chlorophylls is much faster than the primary charge separation. This model assumes a dynamic equilibrium between the excited and the primary radical pair states, and therefore takes into account the charge recombination reaction owing to which the charge stabilization is also reflected in a decay component in the fluorescence. Therefore, the radical pair equilibrium model assumes that there has to be a quenching route into the antenna by the closed RC that should shorten the Fm lifetime. This model was recently brought into question by an analysis of the higher plant RCII structure (52). The distances between the core antennae chlorophylls were found to be too large to satisfy the key assumptions of the radical pair equilibrium model. In addition, new experimental evidence has emerged that shows a rather slow energy transfer from the core antenna pigments to the RCII (53,54). Renger and Renger (55,56) proposed a different scenario of events in the RCII, according to which six pigments of the RC complex, P_{D1}, P_{D2}, Chl_{D1}, Chl_{D2}, $Pheo_{D1}$, and $Pheo_{D2}$ are strongly excitonically coupled such that their excited singlet states are partially delocalized. Therefore, the lowest excited singlet state in RCII was proposed to correspond to the electronically excited complex $^1(P_{D1}P_{D2}Chl_{D1}Chl_{D1}Phaeo_{D1}Phaeo_{D2})^*$, with the largest contribution from $^1Chl_{D1}^*$ rather than (P_{D1}-P_{D2}). The energy gaps between exciton levels are assumed to be small, so at room temperature the excitation is spread 10–30% throughout the six RC pigments. According to this model, there is no reversible charge separation, and therefore when the RCII is closed, the photosystem lifetime is determined solely by the state of the antenna. To our knowledge, our new data provide the first direct evidence that the newer PSII model is correct, and the Holzwarth model, assuming the presence of quenching by the closed RCII, must be given a critical review. Moreover, our findings cast serious doubts on the validity of the two NPQ quenching sites model put forward by Holzwarth and co-workers (33), which was derived solely from the fluorescence lifetime analysis based on the excited-state radical pair equilibrium model.

The reduction in the Fm fluorescence lifetime is also consistent with the fact that the LHCII fluorescence lifetime in liposomes at high protein/lipid ratios, similarly to those of the native membrane, is not 4 ns, as for isolated trimers, but rather is slightly lower than 2 ns (41). The low-temperature fluorescence emission spectrum of LHCII incorporated into liposomes was very similar to one obtained in this study (Fig. 4 *C*). The emission from RCII complexes, which in control thylakoids partially overlapped with the antenna component, was almost absent in treated membranes. This observation allowed us to better analyze the low-temperature fluorescence of LHCII and to identify a shoulder at 700 nm, a typical feature of aggregation of this complex. The finding of aggregated and partially quenched states of LHCII in the photosynthetic membrane confirms our earlier hypothesis regarding the oligomerization and dissipation state of LHCII in vivo (7,47). It was previously argued that the lack of a fluorescence increase after phosphorylation and detachment of LHCII indicates that LHCII must be in a somewhat quenched state (49).

The second important finding of this work is that not only was the antenna fluorescence lifetime under the conditions of dark-adapted leaves (Fm) in the treated plants the same as that observed for the control, the average fluorescence lifetime in the presence of NPQ, Fm′, was also similar to that of the control. Indeed, despite a very strong reduction in the concentration of RCIIs, lincomycin-treated plants possess NPQ that must be driven by a similar extent of ΔpH, generated by the remaining electron transfer chain. This ΔpH must be comparable to that of the control, because the de-epoxidation efficiency, a factor that depends on the ΔpH, was almost the same as in the control plants. Despite the similar levels of PsbS protein (Fig. 1), NPQ was even higher in the lincomycin-treated plants with a very strong quenching, below Fo level, suggesting that it originated from within the peripheral antenna. Indeed, we found that the remaining RCs in the treated plants were largely detached from the large peripheral LHCII antenna, and therefore could not possibly play any role in NPQ. The observed increase in NPQ is consistent with previous observations from plants with a reduced size of the peripheral LHCII antenna. Indeed, plants grown under intermittent light or mutants lacking chlorophyll *b* were reported to possess lower levels of NPQ, suggesting that the peripheral LHCII is largely involved in photoprotection (29,30). One interesting NPQ feature in the treated plants is that the quenching recovered much more slowly than in the control leaves. NPQ recovery strongly depends on the presence of zeaxanthin/de-epoxidation (7). However, the de-epoxidation state in both types of plants was similar. This observation suggests that factors other than the zeaxanthin or PsbS protein, which was recently shown to affect the lateral dynamics of LHCII (58), affected NPQ recovery in the treated plants. Indeed, our recent work showed that a lateral reorganization of the outer antenna, LHCII, as well as core PSII, is required for establishment of the NPQ state (59). It is possible that PSII core complexes assist the membrane remodeling back into the unquenched, efficient state by reorganizing LHCII antenna around them. A strong reduction in RCII in lincomycin-treated plants could simply reduce the fast restoration of NPQ because large clusters of LHCII aggregates would require some time to disassemble, despite the presence of PsbS protein. Hence, the fine balance and dynamic interactions among the core PSII complex, LHCII complexes, and PsbS are emerging as a focal point in research on the regulation of the light-harvesting function

of the photosynthetic membrane. This work provides evidence that the peripheral part of the LHCII antenna plays a key role in photosynthetic function, which is vital for plant productivity and survival.

SUPPORTING MATERIAL

Supplemental data, including a table and four figures, and Materials and Methods are available at http://www.biophysj.org/biophysj/supplemental/S0006-3495(12)00556-5.

We thank Anna M. Yeates for a careful reading of the manuscript.

This work was supported by research and equipment grants from the Biotechnology and Biological Sciences Research Council and the Engineering and Physical Sciences Research Council (A.V.R.), an EU FP7 Marie Curie HARVEST network grant (A.V.R.), and a short-term visiting fellowship from the Federation of the Societies of Biochemistry and Molecular Biology (S.J.).

REFERENCES

1. Allen, J. F., W. B. M. de Paula, …, J. Nield. 2011. A structural phylogenetic map for chloroplast photosynthesis. *Trends Plant Sci.* 16: 645–655.
2. Kouřil, R., J. P. Dekker, and E. J. Boekema. 2012. Supramolecular organization of photosystem II in green plants. *Biochim. Biophys. Acta.* 1817:2–12.
3. Eberhard, S., G. Finazzi, and F. A. Wollman. 2008. The dynamics of photosynthesis. *Annu. Rev. Genet.* 42:463–515.
4. Allen, J. F. 2003. The function of genomes in bioenergetics organelles. *Philos. Trans. R. Soc. Lond. B.* 358:19–25.
5. Allen, J. F., and T. Pfannschmidt. 2000. Balancing the two photosystems: photosynthetic electron transfer governs transcription of reaction centre genes in chloroplasts. *Philos. Trans. R. Soc. Lond. B Biol. Sci.* 355:1351–1359.
6. Barber, J., and B. Andersson. 1992. Too much of a good thing: light can be bad for photosynthesis. *Trends Biochem. Sci.* 17:61–66.
7. Ruban, A. V., M. P. Johnson, and C. D. P. Duffy. 2012. The photoprotective molecular switch in the photosystem II antenna. *Biochim. Biophys. Acta.* 1817:167–181.
8. Ohad, I., D. J. Kyle, and C. J. Arntzen. 1984. Membrane protein damage and repair: removal and replacement of inactivated 32-kilodalton polypeptides in chloroplast membranes. *J. Cell Biol.* 99:481–485.
9. Baena-González, E., and E.-M. Aro. 2002. Biogenesis, assembly and turnover of photosystem II units. *Philos. Trans. R. Soc. Lond. B Biol. Sci.* 357:1451–1459, discussion 1459–1460.
10. Aro, E.-M., I. Virgin, and B. Andersson. 1993. Photoinhibition of Photosystem II. Inactivation, protein damage and turnover. *Biochim. Biophys. Acta.* 1143:113–134.
11. Tyystjärvi, E., and E.-M. Aro. 1996. The rate constant of photoinhibition, measured in lincomycin-treated leaves, is directly proportional to light intensity. *Proc. Natl. Acad. Sci. USA.* 93:2213–2218.
12. Matsubara, S., and W. S. Chow. 2004. Populations of photoinactivated photosystem II reaction centers characterized by chlorophyll a fluorescence lifetime in vivo. *Proc. Natl. Acad. Sci. USA.* 101:18234–18239.
13. Sarvikas, P., T. Tyystjärvi, and E. Tyystjärvi. 2010. Kinetics of prolonged photoinhibition revisited: photoinhibited Photosystem II centres do not protect the active ones against loss of oxygen evolution. *Photosynth. Res.* 103:7–17.
14. Bachmann, K. M., V. Ebbert, …, B. Demmig-Adams. 2004. Effects of lincomycin on PSII efficiency, non-photochemcial quenching, D1 protein and xanthophyll cycle during photoinhibition and recovery. *Funct. Plant Physiol.* 31:803–813.
15. Sárvári, Ė., G. Halász, …, F. Láng. 1976. Effect of lincomycin on the greening process in bean (*Phaseolus vulgaris*) leaves. *Plant Physiol.* 36:187–192.
16. Mulo, P., S. Pursiheimo, …, E. M. Aro. 2003. Multiple effects of antibiotics on chloroplast and nuclear gene expression. *Funct. Plant Biol.* 30:1097–1103.
17. Nayirtai, P., Ė. Sárvári, …, F. Láng. 1994. Organization of thylakoid membranes in low-light grown maize seedlings – effect of lyncomycin treatment. *J. Plant Physiol.* 144:370–375.
18. Gáspár, L., Ė. Sárvári, …, Z. Szigeti. 2006. Presence of 'PSI free' LHCI and monomeric LHCII and subsequent effects on fluorescence characteristics in lincomycin treated maize. *Planta.* 223:1047–1057.
19. Bradford, M. M. 1976. A rapid and sensitive method for the quantitation of microgram quantities of protein utilizing the principle of protein-dye binding. *Anal. Biochem.* 72:248–254.
20. Ruban, A. V., S. Solovieva, …, P. Horton. 2006. Plasticity in the composition of the light harvesting antenna of higher plants preserves structural integrity and biological function. *J. Biol. Chem.* 281:14981–14990.
21. Porra, R. J., W. A. Thompson, and P. E. Kriedemann. 1989. Determination of accurate extinction coefficients and simultaneous-equations for assaying chlorophyll-*a* and chlorophyll-*b* extracted with 4 different solvents—verification of the concentration of chlorophyll standards by atomic-absorption spectroscopy. *Biochim. Biophys. Acta.* 975: 384–394.
22. Ruban, A. V., A. J. Young, …, P. Horton. 1994. The effects of illumination on the xanthophyll composition of the photosystem II light harvesting complexes of spinach thylakoid membranes. *Plant Physiol.* 104:227–234.
23. Weis, E. 1985. Chlorophyll fluorescence at 77 K in intact leaves: characterization of a technique to eliminate artifacts related to self-absorption. *Photosynth. Res.* 6:73–86.
24. Jurić, S., K. Hazler-Pilepić, …, H. Fulgosi. 2009. Tethering of ferredoxin:$NADP^+$ oxidoreductase to thylakoid membranes is mediated by novel chloroplast protein TROL. *Plant J.* 60:783–794.
25. Caffarri, S., S. Frigerio, …, R. Bassi. 2005. Differential accumulation of Lhcb gene products in thylakoid membranes of *Zea mays* plants grown under contrasting light and temperature conditions. *Proteomics.* 5:758–768.
26. Yakushevska, A. E., W. Keegstra, …, P. Horton. 2003. The structure of photosystem II in *Arabidopsis*: localization of the CP26 and CP29 antenna complexes. *Biochemistry.* 42:608–613.
27. Belgio, E., A. P. Casazza, …, R. C. Jennings. 2010. Band shape heterogeneity of the low-energy chlorophylls of CP29: absence of mixed binding sites and excitonic interactions. *Biochemistry.* 49:882–892.
28. Malkin, S., P. A. Armond, …, D. C. Fork. 1981. Photosystem II photosynthetic unit sizes from fluorescence induction in leaves: correlation to photosynthetic capacity. *Plant Physiol.* 67:570–579.
29. Jahns, P., and H. Krause. 1994. Xanthophyll cycle and energy dependent fluorescence quenching in leaves from pea plants grown under intermittent light. *Planta.* 192:176–182.
30. Hartel, H., H. Lokstein, …, B. Rank. 1996. Kinetic studies on the xanthophyll cycle in barley leaves: influence of antenna size and relations to nonphotochemical chlorophyll fluorescence quenching. *Plant Physiol.* 110:471–482.
31. Johnson, M. P., and A. V. Ruban. 2010. *Arabidopsis* plants lacking PsbS protein possess photoprotective energy dissipation. *Plant J.* 61: 283–289.
32. Miloslavina, Y., A. Wehner, …, A. R. Holzwarth. 2008. Far-red fluorescence: a direct spectroscopic marker for LHCII oligomer formation in non-photochemical quenching. *FEBS Lett.* 582:3625–3631.
33. Holzwarth, A. R., Y. Miloslavina, …, P. Jahns. 2009. Identification of two quenching sites active in the regulation of photosynthetic light-harvesting studied by time-resolved fluorescence. *Chem. Phys. Lett.* 483:262–267.

34. Richter, M., R. Goss, …, A. R. Holzwarth. 1999. Characterization of the fast and slow reversible components of non-photochemical quenching in isolated pea thylakoids by picosecond time-resolved chlorophyll fluorescence analysis. *Biochemistry.* 38:12718–12726.

35. Gilmore, A. M., T. L. Hazlett, and Govindjee. 1995. Xanthophyll cycle-dependent quenching of photosystem II chlorophyll a fluorescence: formation of a quenching complex with a short fluorescence lifetime. *Proc. Natl. Acad. Sci. USA.* 92:2273–2277.

36. Gilmore, A. M., V. P. Shinkarev, …, G. Govindjee. 1998. Quantitative analysis of the effects of intrathylakoid pH and xanthophyll cycle pigments on chlorophyll *a* fluorescence lifetime distributions and intensity in thylakoids. *Biochemistry.* 37:13582–13593.

37. Vasil'ev, S., and D. Bruce. 1998. Nonphotochemical quenching of excitation energy in photosystem II. A picosecond time-resolved study of the low yield of chlorophyll *a* fluorescence induced by single-turnover flash in isolated spinach thylakoids. *Biochemistry.* 37: 11046–11054.

38. Johnson, M. P., and A. V. Ruban. 2009. Photoprotective energy dissipation in higher plants involves alteration of the excited state energy of the emitting chlorophyll in the light harvesting antenna II (LHCII). *J. Biol. Chem.* 284:23592–23601.

39. Müller, M. G., P. Lambrev, …, A. R. Holzwarth. 2010. Singlet energy dissipation in the photosystem II light-harvesting complex does not involve energy transfer to carotenoids. *ChemPhysChem.* 11:1289–1296.

40. Johnson, M. P., A. Zia, …, A. V. Ruban. 2010. Effect of xanthophyll composition on the chlorophyll excited state lifetime in plant leaves and isolated LHCII. *Chem. Phys.* 373:23–32.

41. Moya, I., M. Silvestri, …, R. Bassi. 2001. Time-resolved fluorescence analysis of the photosystem II antenna proteins in detergent micelles and liposomes. *Biochemistry.* 40:12552–12561.

42. Belgio, E., G. Tumino, …, R. C. Jennings. 2012. Reconstituted CP29: multicomponent fluorescence decay from an optically homogeneous sample. *Photosynth. Res.* 111:53–62.

43. Pandit, A., N. Shirzad-Wasei, …, W. J. de Grip. 2011. Assembly of the major light-harvesting complex II in lipid nanodiscs. *Biophys. J.* 101:2507–2515.

44. van Dorssen, R. J., J. J. Plijter, …, H. J. van Gorkom. 1987. Spectroscopic properties of chloroplast grana membranes and of the core of photosystem II. *Biochim. Biophys. Acta.* 890:134–143.

45. Andrizhiyevskaya, E. G., A. Chojnicka, …, J. P. Dekker. 2005. Origin of the F685 and F695 fluorescence in photosystem II. *Photosynth. Res.* 84:173–180.

46. Wientjes, E., and R. Croce. 2011. The light-harvesting complexes of higher-plant Photosystem I: Lhca1/4 and Lhca2/3 form two red-emitting heterodimers. *Biochem. J.* 433:477–485.

47. Ruban, A. V., and P. Horton. 1994. Spectroscopy of non-photochemical and photochemical quenching of chlorophyll fluorescence in leaves; evidence for a role of the light harvesting complex of photosystem II in the regulation of energy dissipation. *Photosynth. Res.* 40:181–190.

48. Ruban, A. V., A. J. Young, and P. Horton. 1996. Dynamic properties of the minor chlorophyll a/b binding proteins of photosystem II, an in vitro model for photoprotective energy dissipation in the photosynthetic membrane of green plants. *Biochemistry.* 35:674–678.

49. Ruban, A. V., and M. P. Johnson. 2009. Dynamics of higher plant photosystem cross-section associated with state transitions. *Photosynth. Res.* 99:173–183.

50. Holzwarth, A. R., M. G. Müller, …, M. Rögner. 2006. Kinetics and mechanism of electron transfer in intact photosystem II and in the isolated reaction center: pheophytin is the primary electron acceptor. *Proc. Natl. Acad. Sci. USA.* 103:6895–6900.

51. Miloslavina, Y., M. Szczepaniak, …, A. R. Holzwarth. 2006. Charge separation kinetics in intact photosystem II core particles is trap-limited. A picosecond fluorescence study. *Biochemistry.* 45: 2436–2442.

52. Loll, B., J. Kern, …, J. Biesiadka. 2005. Towards complete cofactor arrangement in the 3.0 A resolution structure of photosystem II. *Nature.* 438:1040–1044.

53. Broess, K., G. Trinkunas, …, H. van Amerongen. 2006. Excitation energy transfer and charge separation in photosystem II membranes revisited. *Biophys. J.* 91:3776–3786.

54. Hughes, J. L., E. Krausz, …, H. Riesen. 2005. Probing the lowest energy chlorophyll a states of photosystem II via selective spectroscopy: new insights on P680. *Photosynth. Res.* 84:93–98.

55. Renger, G., and T. Renger. 2008. Photosystem II: the machinery of photosynthetic water splitting. *Photosynth. Res.* 98:53–80.

56. Renger, G. 2010. The light reactions of photosynthesis. *Curr. Biol.* 98:1305–1320.

57. Reference deleted in proof.

58. Goral, T. K., M. P. Johnson, …, C. W. Mullineaux. 2012. Light-harvesting antenna composition controls the macrostructure and dynamics of thylakoid membranes in *Arabidopsis*. *Plant J.* 69:289–301.

59. Johnson, M. P., T. K. Goral, …, A. V. Ruban. 2011. Photoprotective energy dissipation involves the reorganization of photosystem II light-harvesting complexes in the grana membranes of spinach chloroplasts. *Plant Cell.* 23:1468–1479.